

# Mitochondrial and Intrinsic Optical Signals Imaged During Hypoxia and Spreading Depression in Rat Hippocampal Slices

S. BAHAR,<sup>3,5</sup> D. FAYUK,<sup>4,5</sup> G. G. SOMJEN,<sup>1,2</sup> P. G. AITKEN,<sup>1,4,5</sup> AND D. A. TURNER<sup>2,4,5</sup>

<sup>1</sup>Department of Cell Biology, <sup>2</sup>Department of Neurobiology, <sup>3</sup>Department of Physics, and <sup>4</sup>Department of Surgery (Neurosurgery), Duke University; and <sup>5</sup>Durham Veterans Affairs Medical Center, Durham, North Carolina 27710

Received 15 November 1999; accepted in final form 30 March 2000

**Bahar, S., D. Fayuk, G. G. Somjen, P. G. Aitken, and D. A. Turner.** Mitochondrial and intrinsic optical signals imaged during hypoxia and spreading depression in rat hippocampal slices. *J Neurophysiol* 84: 311–324, 2000. During hypoxia in the CA1 region of the rat hippocampus, spreading-depression-like depolarization (hypoxic spreading depression or HSD) is accompanied by both a negative shift of the extracellular DC potential ( $\Delta V_o$ ), and a sharp decrease in light transmittance (intrinsic optical signal or IOS). To investigate alterations in mitochondrial function during HSD and normoxic spreading depression (SD), we simultaneously imaged mitochondrial depolarization, using rhodamine-123 (R123) fluorescence, and IOS while monitoring extracellular voltage. Three major phases of the R123 signal were observed during hypoxia: a gradual, diffuse fluorescence increase, a sharp increase in fluorescence coincident with the HSD-related  $\Delta V_o$ , primarily in the CA1 region, and a plateau-like phase if reoxygenation is delayed after HSD onset, persisting until reoxygenation occurs. Two phases occurred following re-oxygenation: an abrupt and then slow decrease in fluorescence to near baseline and a slow secondary increase to slightly above baseline and a late recovery. Parallel phases of the IOS response during hypoxia were also observed though delayed compared with the R123 responses: an initial increase, a large decrease coincident with the HSD-related  $\Delta V_o$ , and a trough following HSD. After reoxygenation, there occurred a delayed increase in transmittance and then a slow decrease, returning to near baseline. When  $Ca^{2+}$  was removed from the external medium, resulting in complete synaptic blockade, the mitochondrial response to hypoxia did not significantly differ from control (normal  $Ca^{2+}$ ) conditions. In slices maintained in low-chloride (2.4 mM) medium, a dramatic reversal in the direction of the IOS signal associated with HSD occurred, and the R123 signal during HSD was severely attenuated. Normoxic SD induced by micro-injection of KCl was also associated with a decrease in light transmittance and a sharp increase in R123 fluorescence but both responses were less pronounced than during HSD. Our results show two mitochondrial responses to hypoxia: an initial depolarization that appears to be caused by depressed electron transport due to lack of oxygen and a later, sudden, sharp depolarization linked to HSD. The depression of the second, sharp depolarization and the inversion of the IOS in low-chloride media suggest a role of  $Cl^-$ -dependent mitochondrial swelling. Lack of effect of  $Ca^{2+}$ -free medium on the R123 and IOS responses suggests that the protection against hypoxic damage by low  $Ca^{2+}$  is not due to the prevention of mitochondrial depolarization.

## INTRODUCTION

In many areas of the CNS, including the CA1 and fascia dentata regions of the hippocampus, neurons and glial cells

undergo a severe and sudden depolarization when oxygen is withdrawn (Hansen 1985; Somjen et al. 1993). Because of its phenomenological similarity to classical normoxic spreading depression (SD) (Leão 1944, 1947), this response to hypoxia has been termed hypoxic SD-like depolarization or hypoxic spreading depression (HSD). Both SD and HSD are marked by cessation of neural activity, sudden negative shift in extracellular potential  $\Delta V_o$ , severe depolarization of neurons and glia, and drastic redistribution of ions across the membrane. If oxygen is restored in a timely manner, the tissue can recover with no apparent ill effects, but even after a few minutes permanent damage can occur, particularly in hypoxia-sensitive regions such as the CA1 region of the hippocampus. The neural response to hypoxia is complex and poorly understood, but we do know that the duration of HSD and, in particular,  $Ca^{2+}$  entry into neurons during HSD, are both important factors in determining later neuronal survival following hypoxia (Somjen et al. 1993).

Both SD and HSD are accompanied by changes in the optical properties of brain tissue slices, usually referred to as intrinsic optical signals (IOS). The initial response includes a light transmittance increase and a reflectance decrease, indicating reduced scattering of light. Reduced scattering is thought to be linked to cell swelling (Aitken et al. 1999; Kreisman and LaManna 1999; Kreisman et al. 1994; Müller and Somjen 1999). This is followed by a reversal of the IOS, noted as a propagating wave of either a sharp drop in light transmittance or increase of reflectance. This increased scattering moves as a wave through the CA1 region of hippocampal slices (Aitken et al. 1998; Müller and Somjen 1999; Snow et al. 1983). The onset of the  $\Delta V_o$  at any point in the tissue coincides with the arrival of the leading edge of the wave of increased light scattering. The increased scattering is chloride-dependent but, unlike the initial decrease in scattering, is not directly related to cell swelling (Müller and Somjen 1999). Müller and Somjen (1999) have suggested that this second phase may be linked to swelling of mitochondria.

A role for intracellular calcium ( $[Ca^{2+}]_i$ ) in the neural response to ischemia/hypoxia is not surprising given its normally tight regulation and its function as a regulator of many intracellular processes. Interstitial calcium ( $[Ca^{2+}]_o$ ) decreases drastically during SD and HSD, indicating massive uptake into cells (Hansen 1985; Nicholson and Kraig 1981). Withdrawing  $Ca^{2+}$  from brain slices can prevent lasting damage of the tissue

Address for reprint requests: D. A. Turner, Box 3807, Neurosurgery, Duke University Medical Center, Durham, NC 27710 (E-mail: dennis.turner@duke.edu)

The costs of publication of this article were defrayed in part by the payment of page charges. The article must therefore be hereby marked "advertisement" in accordance with 18 U.S.C. Section 1734 solely to indicate this fact.

by periods of hypoxia that would be lethal in preparations maintained in the presence of normal  $[Ca^{2+}]_o$  (Balestrino and Somjen 1986; Roberts and Sick 1988). These and similar observations have led to the conclusion that  $Ca^{2+}$  entry during HSD and the resulting cascade of intracellular reactions are critical early events in acute hypoxic damage (Siesjö 1981; Somjen et al. 1990). Other processes are clearly involved, as hypoxic neurons will eventually die even with  $Ca^{2+}$  removed from the extracellular medium, but the influx of  $Ca^{2+}$  during HSD appears to greatly accelerate neuron damage. The early stages of the response to hypoxia/ischemia are important to understand to assist with development of therapeutic interventions.

As the organelles of oxidative metabolism, mitochondria are expected to be critically involved in the response to hypoxia. Recent reports have revived the idea that mitochondria buffer cytosolic  $Ca^{2+}$  elevations (David et al. 1998). Excess  $Ca^{2+}$  uptake into mitochondria could, however, lead to their injury and therefore eventually to the demise of the host cell (Crompton 1999; Gunter et al. 1994). It has also been reported that elevated  $Ca^{2+}$  can trigger the mitochondrial permeability transition (mPT), and it is suggested that this transition can initiate apoptotic or necrotic cell injury (Crompton 1999; Lemasters et al. 1997). Finally,  $Ca^{2+}$  released from mitochondria has been blamed for delayed elevation of  $[Ca^{2+}]_i$  and consequent injury to the host cell (Grøndahl and Langmoen 1996; Zhang and Lipton 1999). Given that a rise in  $[Ca^{2+}]_i$  is an important part of the neural response to hypoxia and that mitochondrial function is affected by  $[Ca^{2+}]_i$ , it is possible that the effects of  $Ca^{2+}$  entry during HSD are mediated, at least partly, via effects on mitochondria.

In this paper, we investigate the temporal and spatial relationships among mitochondrial depolarization, hypoxia and HSD and SD in hippocampal slices. Mitochondrial depolarization was measured by changes in rhodamine-123 (R123) fluorescence, which is highly specific in tissue culture and isolated mitochondrial studies (Bindokas et al. 1998; Dubinsky and Levi 1998; Duchen 1992; Grouselle et al. 1990; Johnson et al. 1981). The occurrence of either SD or HSD was recorded as the sudden negative shift in extracellular potential,  $\Delta V_o$ , and was also mapped as changes in the IOS. We find that an initial slow, diffuse mitochondrial depolarization is accompanied by a light transmittance increase through most regions of the hippocampus after the imposition of hypoxia. This pre-HSD phase is then followed by the propagation of a sharp, wavelike increase in fluorescence associated with the onset of HSD and subsequent spread into some regions. In stratum radiatum of CA1, the rapid, wavelike R123 signal is found to coincide with a sharp decrease in light transmittance and with  $\Delta V_o$ . In some experiments, the mitochondrial depolarization extended into regions that did not undergo a light transmittance decrease. Additionally, there was little effect of removing  $Ca^{2+}$  from the bath on the hypoxic R123 fluorescence response as well as on IOS. Normoxic SD, induced by KCl injection, also led to an increased R123 fluorescence concurrent with the IOS but less pronounced than that associated with hypoxia.

## METHODS

### *Slice preparation*

Hippocampal tissue slices were prepared from male Sprague-Dawley rats (60–250 g body wt). The rats were anesthetized with diethyl

ether or fluothane (halothane) and decapitated. The brain was rapidly (1–2 min) removed from the skull and placed in chilled artificial cerebrospinal fluid (ACSF, composition defined in the following text) for 1–2 min. One hippocampus was isolated, and transverse 400- $\mu$ m slices were cut with a tissue chopper. These experiments were fully approved by the Institutional Animal Care Committee at Duke University. After preparation, slices were incubated for 15–20 min in 5  $\mu$ g/ml R123 and then transferred to an “Oslo-style” interface chamber in one of two physiology and imaging workstations. The chambers were similar in design, were maintained at  $35 \pm 1^\circ\text{C}$ , were continuously aerated with 95%  $O_2$ -5%  $CO_2$  (400 ml/min), and were perfused with oxygenated ACSF flowing at a rate of 1.5 ml/min. After placement in the interface chamber the slices were allowed to recover for  $\geq 60$  min before viability was assessed by measurement of evoked potentials in the s. radiatum and s. pyramidale. Hypoxia was induced by replacing the 95%  $O_2$ -5%  $CO_2$  atmosphere with 95%  $N_2$ -5%  $CO_2$ , at the same rate.

### *Solutions*

The ACSF contained (in mM) 130 NaCl, 3.5 KCl, 1.25  $NaH_2PO_4$ , 24  $NaHCO_3$ , 1.2  $CaCl_2$ , 1.2  $MgSO_4$ , and 10 dextrose (pH 7.4). Calcium-free medium was identical to ACSF except that no  $CaCl_2$  was added, the concentration of  $MgSO_4$  was 4.8 mM, and 1 mM ethylene glycol-bis( $\beta$ -aminoethyl ether)- $N,N,N'$ -tetraacetic acid (EGTA) was added to chelate any residual  $Ca^{2+}$  remaining in the extracellular space. In low-chloride medium, KCl and NaCl were replaced with  $KCH_3SO_4$  and  $NaCH_3SO_4$ .

### *R123 staining*

For dye staining, slices were incubated in continuously oxygenated ACSF containing 5  $\mu$ g/ml rhodamine-123 (Molecular Probes) at room temperature. R123 was diluted 1:2000 from a 10 mg/ml stock in 95% EtOH. Slices were left in the staining solution for 15–20 min and briefly washed in dye-free ACSF before being placed in the interface chamber. R123 enters cells and partitions across the mitochondrial membranes according to the membrane potential. Under normal conditions, most of the dye is inside mitochondria and, due to self-quenching, the overall fluorescence is low. When the mitochondria depolarize, dye leaves the mitochondria and enters the cytoplasm, and reduced quenching results in greater overall fluorescence. To verify that R123 fluorescence was in fact due to mitochondrial depolarization, we recorded R123 fluorescence in the presence and absence of carbonyl cyanide  $p$ (trifluoromethoxy)phenyl-hydrazone (FCCP), a highly effective uncoupler of mitochondrial oxidative phosphorylation (Heytler 1980). FCCP was administered either through the bath (1  $\mu$ M FCCP in ACSF) or by injecting it (100  $\mu$ M) into the s. radiatum region of CA1 either in separate slices or after another manipulation. As also reported by Bindokas et al. (1998), we verified that R123 fluorescence is significantly enhanced during FCCP treatment. The maximal R123 fluorescence under these conditions was comparable to, though no larger than, that observed during prolonged hypoxic conditions. Since the penetration of both the R123 and FCCP was variable between slices, the absolute values of the fluorescence induced by all of the conditions described here as well as FCCP differed, so the magnitude of the fluorescence could not be directly compared. However, the FCCP fluorescent response was equivalent to that observed during the most severe condition in our experiments, prolonged hypoxia (for  $\leq 10$  min).

### *KCl micro-injections*

Normoxic SD was triggered with a brief high-pressure (20–60 lb/in<sup>2</sup>; 20–100 ms) micro-injection of 1 M KCl into CA1 s. radiatum via a glass micropipette (tip diameter  $\leq 5 \mu$ m) connected to a Pico-spritzer (General Valve). In each experiment, the pulse pressure and duration were adjusted to find the minimal values capable of evoking

reproducible SD in one of the slices for a given micropipette. The same pulse through the same pipette was then used to inject KCl into other slices. For data analysis, we used only the first normoxic SD induced in each slice, with the requirement that full recovery of the excitatory postsynaptic potential (EPSP) amplitude was obtained during the first 15 min after SD. The recording electrode was placed in the s. radiatum of CA1 between the KCl injection pipette and CA3 region at  $\sim 500 \mu\text{m}$  from the injection site.

### Voltage recording

Extracellular measurements of evoked and DC potentials were made using thin-walled, single-barreled borosilicate glass microelectrodes (World Precision Instruments) with a tip resistance of  $\sim 5 \text{ M}\Omega$ . The electrodes were filled with 150 mM NaCl.

### Imaging

Slices in the interface chambers were imaged through either a Nikon upright microscope (UM-2) with a compound lens ( $\times 4$ ) or a Nikon dissecting microscope (SMZ-U), using a linear, cooled 12-bit charge-coupled device (CCD) camera. Because of the two different configurations, epifluorescence was used in one and transmission fluorescence was used in the other. These two separate imaging workstations, though similar in most respects, did show minor differences between some of the imaging and fluorescence results, but in all significant respects the results were highly consistent. Two 12-bit cameras were used: a Princeton Instruments PentaMAX system, with  $1,024 \times 512$  frame transfer CCD (at  $-35^\circ\text{C}$ ) or a Cooke Instruments Sencicam, with  $640 \times 480$  interline CCD (at  $-15^\circ\text{C}$ ). Images were taken once every 1–2 s (50–500 ms exposure for each image). The images were usually acquired as  $2 \times 2$  binned images, reducing the effective spatial resolution to either  $256 \times 256$  or  $320 \times 240$  pixels. The direct digital images for both cameras were transferred to the host computer and stored as 12-bit files. Each binned pixel corresponded to a slice region of  $6\text{--}16 \mu\text{m}^2$  depending on the magnification used.

For imaging of R123 fluorescence, slices were either epi- or *trans*-illuminated, using excitation light consisting of wavelengths centered at either 485 nm (with a long-pass emission filter 520 nm), or 535 nm (using a long-pass 580-nm emission filter). Both (the longer and shorter wavelength) pairs of excitation/emission filters gave a large fluorescence signal due to the wide bandwidth of R123 excitation. Emitted light was also passed through an infrared filter (cutoff at 700 nm) to eliminate extraneous near infrared light. To assess whether there was intrinsic slice fluorescence (using the preceding wavelengths), unstained slices were imaged in the same manner using hypoxia; no intrinsic slice fluorescence could be detected at the frequencies used for the R123 fluorescence with the intensity of light normally used for excitation. Likewise using both epifluorescence and transmission fluorescence, we assessed whether there was any bleed-through of excitation light past the blocking filters, and this was  $< 1\%$  of our measured signals, using representative light intensities.

For imaging of the IOS, the chamber was illuminated from below using a stabilized xenon arc lamp. The transmission light source was filtered to a narrowband-pass centered at 650 nm to minimize any direct R123 excitation. This combination of light sources allowed alternating images using the same filter system and camera by alternating only the excitation source since the direct transmitted light for the intrinsic optical signal (IOS) determination passed directly through the emission filters for the fluorescence. The optimal transmitted light intensity was  $\sim 10\text{--}15$  times less than the intensity of light used for R123 excitation, again minimizing any unexpected R123 fluorescence contribution to the intrinsic optical signal. Thus it should be emphasized that the alternate measurements of IOS were independent of the R123 fluorescence except that the concurrent intrinsic optical changes in the tissue also influence the direct transmission of the R123 excitation and emission light through the tissue. However, the intrinsic optical signal and R123 fluorescence usually responded in

opposite directions (i.e., a decrease in IOS occurring together with an increase in R123 fluorescence), leading to only a small likelihood of significant interaction between the two signals.

### Data analysis

Each series of images was analyzed using regions of interest, generating a series of 12-bit intensity numbers for plotting. Difference images were also calculated for each series, using a control image as a baseline for each further image in the series:  $\Delta I/I = (\text{Image}_n - \text{Image}_{\text{control}})/\text{Image}_{\text{control}}$ . In these difference images, no difference was scaled as a value of 128, while a decrease showed smaller values (to black) and an increase showed larger values (to white). Data were analyzed for statistical significance using *t*-tests and ANOVA where needed. Data are shown as means  $\pm$  SD.

## RESULTS

### Short-term hypoxia

**PHASES OF RESPONSE TO HYPOXIA.** Overall, three major phases of the R123 signal were observed in response to hypoxia: a gradual, diffuse fluorescence increase over much of the slice following the removal of oxygen, lasting several minutes (pre-HSD phase), a sharp increase in fluorescence coincident with the HSD-related  $\Delta V_o$ , occurring primarily in the CA1 region, but also occasionally in the dentate gyrus (HSD phase), and a plateau-like elevation that persists for the duration of hypoxia, if reoxygenation is delayed following the onset of HSD (hypoxic plateau phase). Following reoxygenation there were two additional phases: an abrupt initial decrease in fluorescence followed by a more gradual decrease of R123 signal to near baseline (initial reoxygenation phase) and a late reoxygenation phase dependent on the duration of hypoxia, consisting of a slow delayed increase to above baseline and then a slow recovery toward the rest level. The IOS response to hypoxia was parallel to the R123 signal response but showed some differences in time course: an initial increase, before onset of HSD, coincident with the pre-HSD R123 phase; a large decrease coincident with the HSD-related  $\Delta V_o$  and R123 HSD phase; and a trough following HSD, with a delayed, persistent decrease. On reoxygenation a delayed and often overshooting increase in transmittance occurred, after the R123 signal has returned to baseline, followed by a further late decrease with an eventual return to near baseline, occurring during and after the late reoxygenation R123 phase. The R123 signal more closely followed the reoxygenation of the slice tissue while the intrinsic optical signal responded with a more complex set of phases and more delay following reoxygenation.

Figure 1 shows a series of images that were obtained during a typical hypoxia experiment. The *top image* in each column is an unsubtracted (raw) control image, showing either R123 fluorescence (*left*) or IOS (*right*). All of the subsequent images represent a sequence of R123 fluorescence (*left*) and IOS (*right*) difference images; numbers accompanying each frame indicate the time in seconds following the onset of hypoxia. Note that the images were interleaved so the IOS image is offset by 1 s from the R123 image. Each subtraction or difference image is a result of pixel-by-pixel subtraction of a control image obtained 1 min before hypoxia onset, from the image obtained at the indicated time after hypoxia onset, divided by the control image values ( $\Delta I/I$ ; see figure legend and METHODS for details). The calibration for the image intensity is shown on the *right*, with gray as unchanged and either black or white

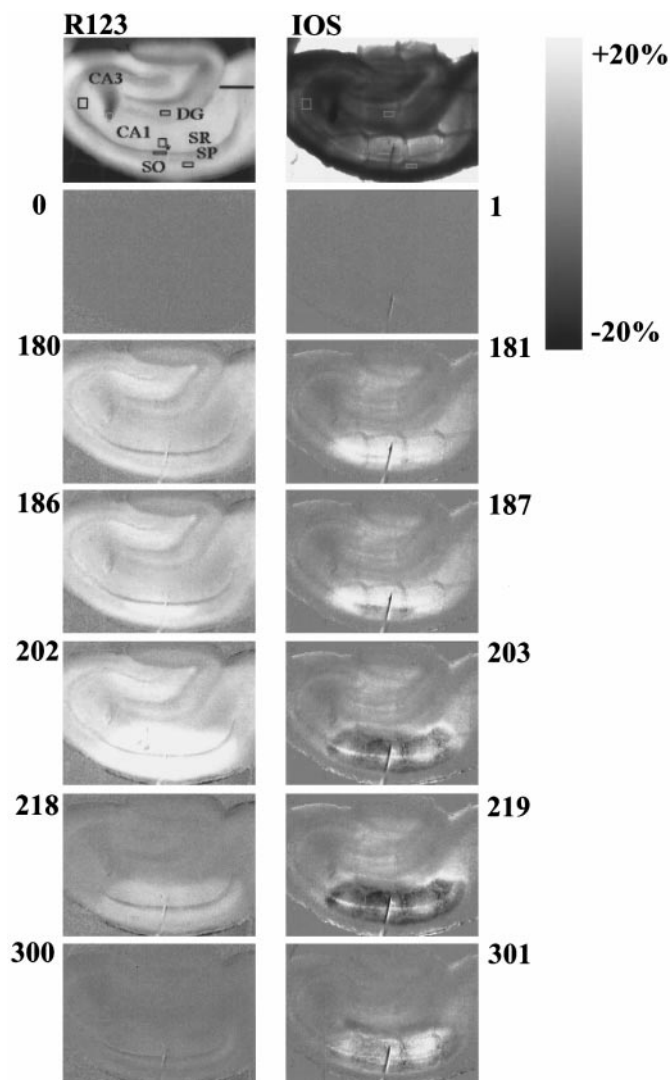


FIG. 1. Frame sequence showing increase of rhodamine-123 (R123) fluorescence (*left column*) and changes in light transmittance [*right column*, intrinsic optical signal (IOS)] of a hippocampal slice, with the stratum radiatum of CA1 particularly involved during hypoxia. The 2 *top frames* show unsubtracted camera images; in the other frames, intensities measured in each pixel were subtracted from corresponding control levels and normalized ( $\Delta/I$ ). Subtracted images are transposed to a gray scale so that pixels with no change are gray, those with fluorescence 20% brighter than the control images are white, and pixels 20% darker are black. Numbers show the time in seconds after the onset of hypoxia. In the *top left image*, regions are labeled [CA1, CA3, dentate gyrus (DG), s. radiatum (SR), s. oriens (SO), and s. pyramidale (SP)]; the white circle indicates the stimulating electrode and the asterisk indicates the extracellular recording electrode. This figure was obtained using transmission fluorescence. Scale bar represents 500  $\mu\text{m}$ .

values as  $\pm 20\%$  difference. Figure 2 shows the time course of R123 fluorescence and IOS in this experiment for the regions of interest (ROIs) marked in the Fig. 1, *top left*.

**PRE-HSD PHASE.** During normal oxygenation and just after onset of hypoxia, no visible changes in either R123 fluorescence or IOS were observed compared with the control images. This baseline is indicated by the uniform gray color throughout the slice in both second images (at 0 and 1 s) and by the baseline values in the plots in Fig. 2. The initial pre-HSD phase of the R123 response began shortly (10–30 s) after the withdrawal of oxygen. This phase consisted of a slow ramp of fluorescence increase occurring widely over the slice (Fig. 1,

*left*, at 180 and 186 s), accompanied by a gradual brightening of the transmitted light signal (*right*, at 181 and 187 s). In contrast to the diffuse R123 fluorescence, the transmittance increase was mostly restricted to the CA1 region (Fig. 1, 181 and 187 s). The average duration of this pre-HSD phase was  $162 \pm 52$  s ( $n = 26$ ), measured in one of the two interface chambers. Once started, this gradual increase of the R123 signal and transmittance continued until either HSD onset or reoxygenation if this was instituted prior to HSD onset (data not shown).

The time course of both the R123 signal and the IOS varied considerably depending on the location of measurement, with CA3 and dentate gyrus (DG) showing considerably different responses from those in the CA1 region, as shown in Fig. 2 for different regions. Figure 2B shows the R123 signal in CA1 s. radiatum by itself, and the arrows point to inflection points for the start of the pre-HSD phase and the onset of the HSD (discussed in the following text). For example, the slope of R123 fluorescence increase during this pre-HSD phase was slightly higher in the CA3 region than in other regions, particularly s. pyramidale in the CA1 region (the slopes are shown in more detail in Table 1, and given as percentage change per second). However, the transmittance values were opposite: a lesser rate was noted in the CA3 region compared with that observed in st. pyramidale of CA1. There did not appear to be a correlation between the duration of the pre-HSD phase and the total extent of the increase of either R123 fluorescence or intrinsic optical signal.

**HSD PHASE.** By images 202/203 of Fig. 1, the HSD has started in the CA1 region, with a marked decrease in the transmission IOS and an increase in the same region in the R123 signal. The sharp increase in R123 fluorescence moved as a wave through CA1, in the same direction and generally overlapping the progressive regions involved with the IOS, as noted in images 218/219. The increased light scattering indicated by the decreased transmittance during HSD (on the order of  $\geq 15\%$ ) would be expected to depress the R123 signal because both the excitation light and the emitted fluorescence are hindered in their passage through tissue. In spite of this expected decrease due to the interaction between the signals, the R123 signal increased significantly in amplitude (ranging from  $32.8 \pm 5.7\%$  for CA1 s. radiatum to  $22.0 \pm 7.7\%$  for CA3 s. radiatum,  $n = 29$  slices), suggesting that the signal would be even larger if there were no interference from the intrinsic optical signal and passive transmission characteristics of the tissue during the peak of the HSD. The peak values for R123 maximal increase during HSD varied both between slices (due to variable loading) and between regions, but CA1 s. radiatum usually showed the most intense response as depicted in Fig. 1. There was also some difference in the absolute maximal change noted between the two chambers used for this study, beyond slice loading of R123 and regional variation. These differences can likely be interpreted as resulting primarily from the differences in illumination intensity in the different experimental setups.

The slopes of the R123 fluorescence increase in various regions (Table 1) were measured for the first 12 s after HSD onset marked by the second arrow in Fig. 2B. This large change at HSD onset indicated a dramatic acceleration of mitochondrial depolarization possibly due to the enhanced metabolic stress of HSD, beyond the pre-HSD hypoxia alone. This increase in the slope (as a ratio of HSD slope/pre-HSD slope)

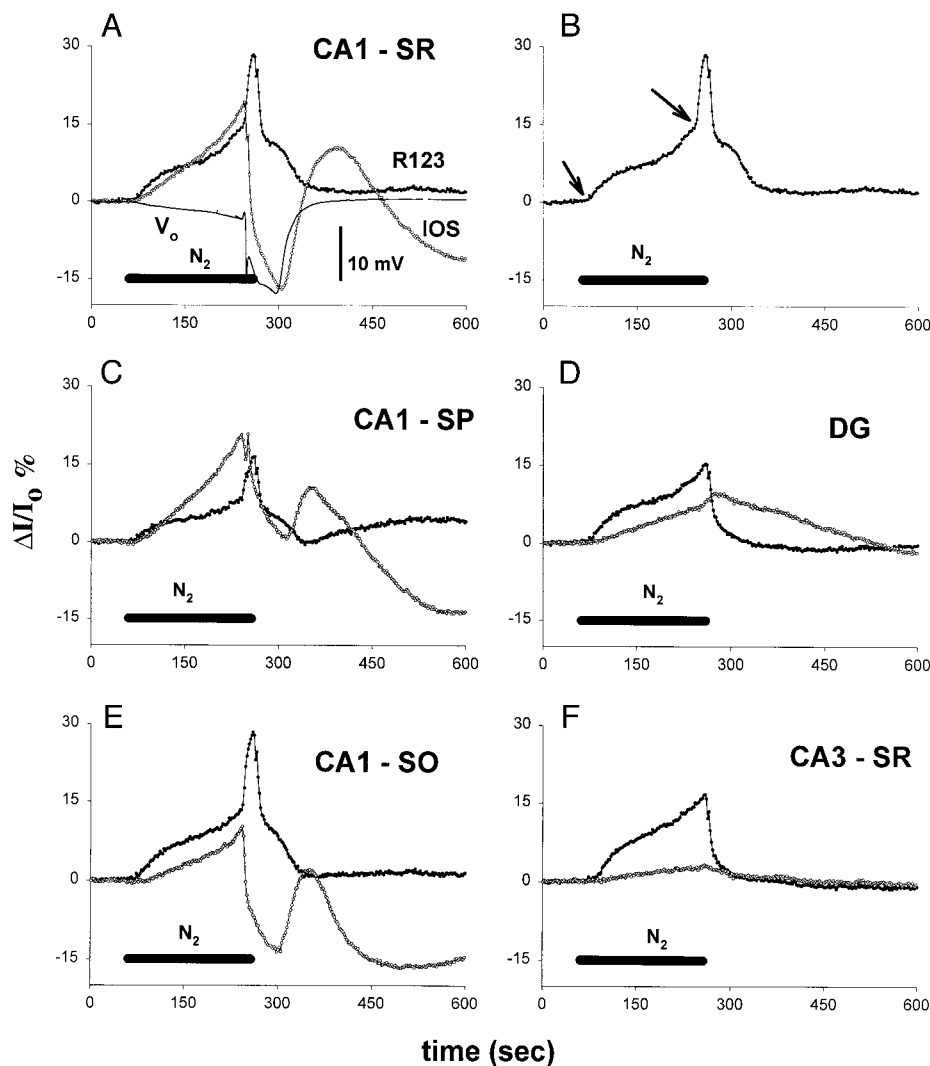


FIG. 2. R123 fluorescence (●) and intrinsic optical signal (○) during and after hypoxia. Each graph shows data from 1 of the boxed regions in the top left frame of Fig. 1. The ordinate scales show the change of fluorescence or transmittance intensity ( $\Delta I$ ) as a percentage of the control level  $I_0$  ( $\Delta I/I_0$ ). A: the extracellular voltage ( $V_o$ ) recorded in s. radiatum is shown as —. The horizontal bars along the x axis indicate the duration of hypoxia. B: the R123 trace from frame A, with  $\rightarrow$  indicating the inflection points between which slopes are calculated (see text). C–F: image analysis of various regions of interest as a function of time. This figure was obtained using transmission fluorescence.

varied from 2.2 [CA3 s. radiatum (st. rad.)] to 17.0 (CA1 st. rad.; Table 1; comparison of slopes for pre-HSD and HSD values significantly different by *t*-test,  $P < 0.001$ ). Oxygen was restored immediately after the onset of the HSD for the example shown in Figs. 1 and 2. However, if hypoxia was not

terminated soon after HSD onset (within 10–20 s), similar IOS and R123 changes were occasionally observed in DG, indicating HSD appearance in this region (data not shown) (but see Balestrino et al. 1989). Although initially the R123 fluorescence change and IOS decrease were very rapid, the response

TABLE 1. R123 fluorescence slopes for phases 1 and 2 of hypoxia response

|                           | CA1              |                 |                 |                 |
|---------------------------|------------------|-----------------|-----------------|-----------------|
|                           | Stratum radiatum | S. pyramidale   | DG Molecular    | CA3 S. Radiatum |
| <b>Hypoxia</b>            |                  |                 |                 |                 |
| Pre-HSD                   | $0.11 \pm 0.08$  | $0.08 \pm 0.07$ | $0.09 \pm 0.07$ | $0.17 \pm 0.09$ |
| HSD                       | $1.43 \pm 0.49$  | $0.84 \pm 0.36$ | $1.46 \pm 0.47$ | $0.27 \pm 0.14$ |
| Ratio HSD/Pre-HSD         | $17.0 \pm 7.5$   | $13.2 \pm 6.6$  | $16.4 \pm 7.8$  | $2.2 \pm 1.7$   |
| <i>n</i> (slices)         | 16               | 16              | 10              | 16              |
| <b>Low CI experiments</b> |                  |                 |                 |                 |
| <b>Control</b>            |                  |                 |                 |                 |
| Pre-HSD                   | $0.17 \pm 0.19$  | $0.16 \pm 0.16$ | $0.16 \pm 0.19$ | $0.22 \pm 0.18$ |
| HSD                       | $1.67 \pm 0.60$  | $1.14 \pm 0.64$ | $1.88 \pm 0.74$ | $0.40 \pm 0.20$ |
| Ratio HSD/Pre-HSD         | $16.7 \pm 8.5$   | $10.8 \pm 5.5$  | $16.5 \pm 12.1$ | $3.5 \pm 2.6$   |
| <b>Low CI</b>             |                  |                 |                 |                 |
| Pre-HSD                   | $0.16 \pm 0.11$  | $0.11 \pm 0.6$  | $0.12 \pm 0.09$ | $0.25 \pm 0.19$ |
| HSD                       | $0.98 \pm 0.78$  | $0.54 \pm 0.37$ | $0.94 \pm 0.92$ | $0.38 \pm 0.20$ |
| Ratio HSD/Pre-HSD         | $6.5 \pm 3.0$    | $5.9 \pm 2.2$   | $9.0 \pm 6.2$   | $2.9 \pm 2.1$   |
| <i>n</i> (slices)         | 5                | 5               | 3               | 5               |

R123, rhodamine-123; DG, dentate gyrus; HSD, hypoxic spreading disease.

slowed down as a peak was reached, particularly for persistent hypoxia (discussed in the following text). During persistent hypoxia, the R123 fluorescence reaches a plateau, and this phase is discussed further in the following text. It is important to note that after HSD onset in CA1 the rates of R123 fluorescence increase were almost unchanged in regions (DG and CA3) not expressing HSD (see Table 1). This point is well illustrated in both the images in Fig. 1 and the plots in Fig. 2: at the time of the large R123 signal increase in all subregions of CA1 the R123 fluorescence continued at the same rate as during the pre-HSD phase in DG and CA3. Interestingly, the extent of IOS decrease during HSD strongly correlated with the degree of R123 fluorescence enhancement, and both effects were maximal in dendritic regions (s. radiatum and s. oriens) of CA1 (and molecular layer of DG) and minimal in the cell body layer (s. pyramidale).

In this example, there is no plateau phase due to the short duration of hypoxia. However, in later examples (Fig. 5) the plateau phase is shown with prolonged hypoxia.

**INITIAL REOXYGENATION PHASE.** Termination of hypoxia led to an abrupt but partial fall of R123 fluorescence in all regions of hippocampal slice, irrespective of the total duration of hypoxia. The example shown in Figs. 1 and 2 indicates the rapid changes occurring in both R123 and IOS immediately following reoxygenation, which occurred directly after the HSD onset. During the first 15 s of reoxygenation, R123 fluorescence decreased more than twofold, indicating a rapid mitochondrial repolarization to the renewed presence of oxygen. At the same time, the IOS continued to decrease slowly in the regions experiencing HSD (CA1) with no direct change in time course. But in those regions in which HSD did not appear (CA3 and DG in Fig. 2), the IOS, which was slightly enhanced during hypoxia, began to recover slowly. The initial rapid reduction of the R123 signal was followed by a slower decrease of fluorescence that lasted roughly until the beginning of IOS recovery, which consisted of a slow return to baseline. At about this time, the DC extracellular potential also started to recover quickly (Fig. 2A). The recovery of IOS in the regions experiencing HSD started with some delay ( $\sim 30$ – $40$  s) after termination of hypoxia (here we describe recovery process after a short-term HSD episode with rapid reoxygenation). Since the R123 signal is reliably linked to restoring oxygen to the tissue, the delay in the IOS likely reflects a recovery process that is ongoing after restoration of oxygen. At the end of this phase, both the R123 and IOS signals were close to baseline values.

**LATE REOXYGENATION PHASE.** Further recovery included a final, late phase of R123 and IOS responses following hypoxia and then reoxygenation. First, there followed a period of concurrent further decrease in the R123 signal toward baseline, and a rapid increase of the IOS, with an overshoot above baseline noted particularly in the CA1 s. radiatum region (Fig. 2A). Next, there occurred a period of a secondary increase of R123 fluorescence above the baseline level, and secondary slow decrease of the IOS, lasting  $\sim 3$ – $4$  min. This secondary increase is minor in Fig. 2A and more apparent in Fig. 2C, in the CA1 s. pyramidale region, and was partially dependent on the duration of the hypoxic conditions. In this particular example, there was rapid reoxygenation so the secondary late increase in the R123 signal was minor compared with longer durations of hypoxia. Eventually there was a final recovery to

near the rest level of both the R123 and IOS signals, which often required 20–30 min (data not shown). This time for recovery coincided with recovery of synaptic field potentials (not shown).

#### Variations in short-term hypoxic response

In 5 of 47 experiments we observed a somewhat different pattern of response, which included a large R123 signal in regions that did not show a drop in IOS, particularly in the CA3 region. Images for this less common outcome are shown as a montage in Fig. 3, and the time course of ROIs for the CA1 s. radiatum and CA3 s. radiatum for one such typical experiment are shown in Fig. 4. Both the images and the plots reveal a robust biphasic (gradual pre-HSD increase followed by rapid HSD) R123 signal in both CA1 and CA3, though the expected IOS decrease was not observed in CA3. In the more typical short-term hypoxia responses demonstrated in Figs. 1 and 2, the large, rapid R123 signal present at the start of HSD onset was consistently colocalized with a large, decreasing IOS.

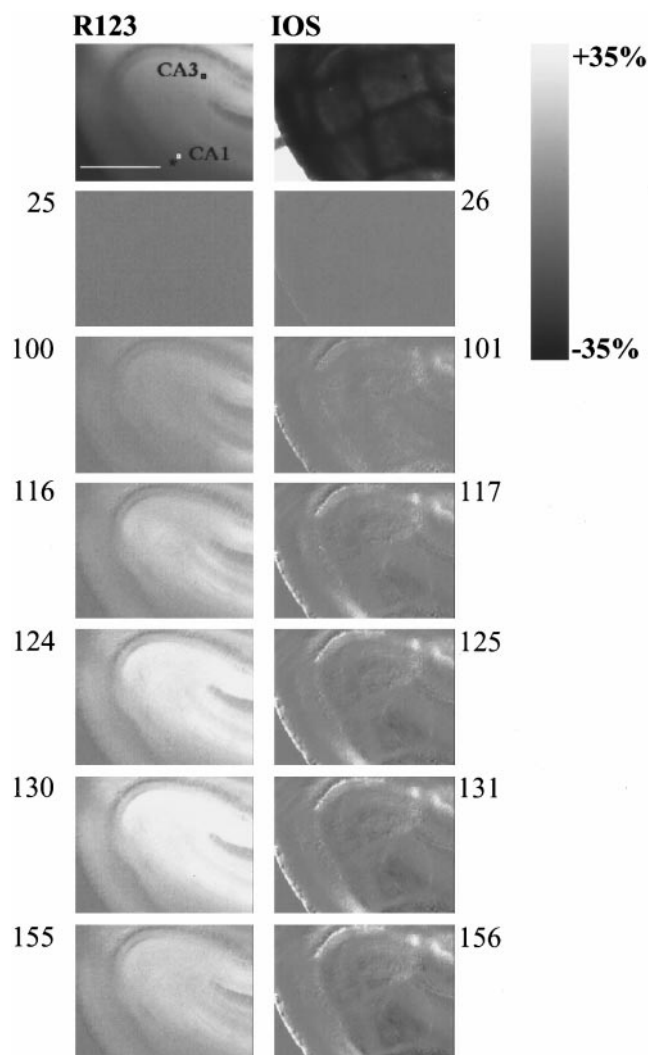


FIG. 3. Frame sequence showing changes of R123 fluorescence (*left column*) and light transmittance (*right column*) in the s. radiatum of CA1, DG, and s. radiatum of CA3, during hypoxia. The *top 2 frames* are unsubtracted images, those *below* were processed similarly to Fig. 1 but from another slice and with the gray scale extending from  $-35$  to  $35\%$ . This figure was obtained using epi-fluorescence. Scale bar represents  $500 \mu\text{m}$ .

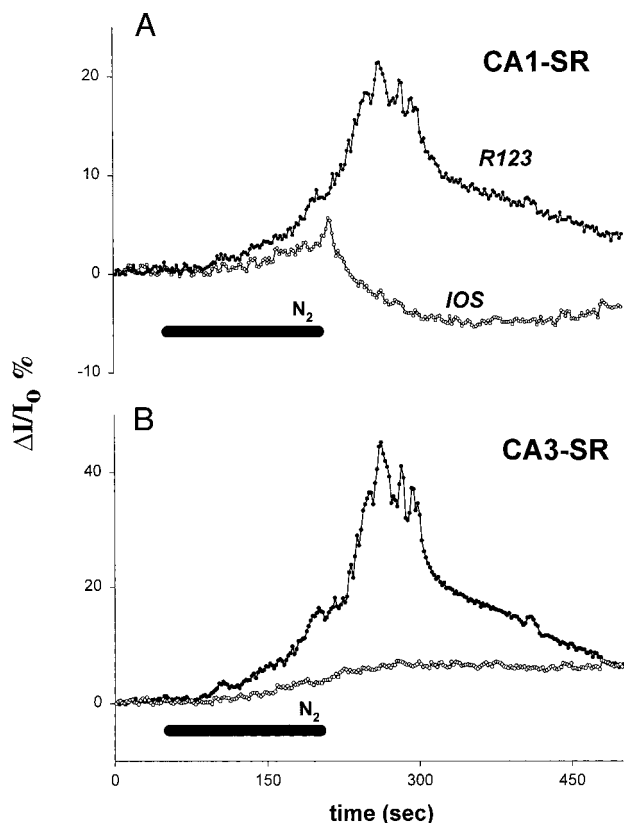


FIG. 4. Time course of R123 fluorescence (closed circles) and light transmittance (open circles) in s. radiatum of CA1 and CA3 during an episode of hypoxia in a different slice than illustrated in Figs. 1 and 2 (boxed regions in Fig. 3). As in Fig. 2, the scales show the change of fluorescence or transmittance intensity ( $\Delta I$ ) as a percentage of the control level  $I_0$  ( $\Delta I/I_0$ ). This figure was obtained using epi-fluorescence.

As discussed in the preceding text, the presence of the IOS decrease (a lessened transmittance through the tissue) likely led to a decline in the overall observed R123 response, but the interaction between the two independent signals could be more complex than just a linear summation. In contrast, the example shown in Figs. 3 and 4 demonstrates a minimal concurrent IOS change together with a large, rapid R123 signal, indicating that the R123 signal clearly does occur in the absence of a large, negative IOS response. Thus the summation in the more typical experiments may approach a linear combination of the two effects, reducing the effective, imaged R123 fluorescence signal to less than the actual generated signal.

#### Multiple short hypoxic episodes

In some cases, short-term hypoxic treatments (with rapid reoxygenation after HSD occurrence) were repeatedly applied to the same slice, though allowing complete recovery of the evoked, field synaptic potentials between episodes. Recovery was indicated by return to the control amplitude of the field EPSP, usually occurring  $\geq 30$  min after onset of the previous HSD episode, associated with full recovery of the intrinsic optical signal. For such successive hypoxia treatment, the R123 and IOS responses were very similar (data not shown) across all trials. We have administered up to six successive short-term hypoxic treatments in the same slice, but on each trial, there was a slight but progressive reduction of the duration of the

pre-HSD phase without significant slope changes of either the pre-HSD or HSD phases (data not shown). For example, comparison of the R123 fluorescence slopes (pre-HSD and HSD slopes) in s. radiatum of CA1 from pairs of successive hypoxic trials (next/preceding) revealed no significant difference, averaging  $1.14 \pm 0.32$  and  $1.00 \pm 0.12$  for pre-HSD and HSD phases, respectively (mean  $\pm$  SD, 21 comparisons in 16 slices; compare to Table 1). This observed consistency in subsequent short-term episodes is critical when performing multiple hypoxia treatments under different conditions in the same slice, to be described in the following text. Typical protocols for such experiments consisted of alternation of hypoxic trials in control and experimental ACSF conditions (see following text), and then the pairs of successive responses at different conditions were analyzed. These results confirm that analysis of successive short-term hypoxic episodes is a valid scheme to assess treatment effects.

#### Prolonged hypoxia

The short-term hypoxia conditions described in the preceding text focused on reoxygenation within 20 s following onset of HSD as determined by the extracellular recording of  $\Delta V_o$  in CA1 s. radiatum. This paradigm reliably resulted in complete recovery of the field synaptic potential within 30–60 min. However, after long-term (up to  $\sim 10$  min) hypoxia, slices fail to recover electrical function as determined by the absence of field synaptic potentials even after 1 h of recovery following HSD occurrence (data not shown). Moreover recovery of IOS was poor following such prolonged hypoxia. However, R123 fluorescence recovers rapidly after reoxygenation, irrespective of hypoxia duration  $\leq 10$  min. Plots of typical R123 and IOS responses in s. radiatum of CA1 during successive short- and long-term hypoxic treatments applied in the same slices are presented in Fig. 5. With extension of hypoxia beyond the immediate HSD phase, R123 fluorescence tended to reach a plateau of increased fluorescence after  $\sim 1$ –3 min, which is designated the hypoxic plateau phase. This plateau-like level occurred in slice regions even if there was no direct involvement in HSD propagation. However, the maximal relative increase and plateau levels of R123 fluorescence were substantially larger in regions that experienced HSD. This hypoxic plateau level was not necessarily completely stable and could either slowly increase or decrease, depending on the specific region of the slice. The maximal levels for the hypoxic plateau were slightly higher than those noted for the experiments in which rapid reoxygenation was performed, in the range of 30–40%, but most of the R123 response occurred within the first 12–20 s after onset of HSD.

As shown in Fig. 5, the time course for the rapid decrease in R123 fluorescence immediately following reoxygenation (initial reoxygenation phase) did not differ between the short and prolonged hypoxic episodes. The presence of the hypoxic plateau of the R123 signal and its maintenance for  $\leq 10$  min of hypoxia without significant decline strongly suggests that there is little bleaching of the R123 dye or loss of the dye from the cells in the hippocampal slice. Also that the mitochondrial depolarization can rapidly reverse and normalize almost immediately with reoxygenation indicates the likely sustained viability of the mitochondria giving rise to the fluorescent signal. The rapid resumption of mitochondrial function suggests that the observed mitochondrial de-

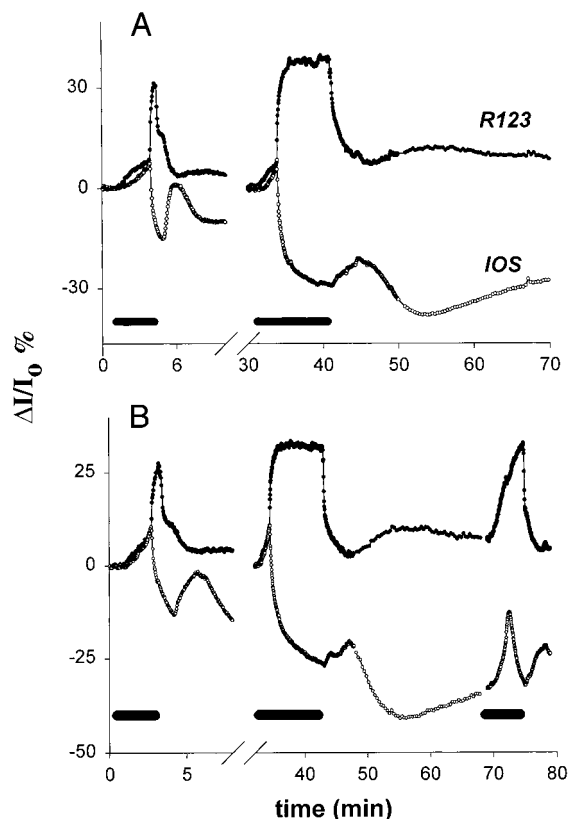


FIG. 5. Effects of prolonged and repeated hypoxia on R123 fluorescence (closed circles) and on light transmittance (open circles). The y axis shows both the change of R123 fluorescence and transmittance intensity ( $\Delta I$ ) as a percentage of the control level  $I_0$ . Horizontal bars show the duration of hypoxia. Data in A and B are from 2 different slices. Note that the x axis shows time in minutes. This figure was obtained using transmission fluorescence.

polarization is reversible in spite of profound mitochondrial depolarization after  $\leq 10$  min of hypoxia and argues against any form of irreversible mitochondrial alteration. The rapid normalization of the R123 fluorescence also appears to imply a real recovery of mitochondrial potential as shown by the ability of a subsequent (3rd) hypoxia to again cause a large increase in R123 fluorescence of amplitude similar to previous episodes (Fig. 5B). Since the absolute maximum R123 fluorescence does not appear to wane significantly with subsequent episodes of hypoxia, there may be minimal actual cell leakage of the dye or bleaching of the dye with prolonged fluorescence excitation. The rapid reversibility of the mitochondrial signal in spite of the loss of the field potential with prolonged hypoxia also suggests a dissociation between conditions suitable for mitochondrial survival and repolarization versus those necessary for neuronal survival and recovery of electrical activity.

In contrast to the rapidly reversible R123 response with prolonged hypoxia, both the extracellular field potential and IOS showed much less reversibility and recovery (Fig. 5). There was a large, abrupt extracellular shift ( $-25$ -mV peak) associated with the first two HSD events shown in Fig. 5. However, after the second HSD, there was no recovery of the field potential, and the peak extracellular shift on the third HSD was only  $-8$  mV and exhibited a much slower time course. This lack of recovery was mirrored in the intrinsic signal as well since the third HSD began on a much more negative level than the previous two events.

Also, with the longer episodes of hypoxia duration, there appeared a much more pronounced secondary increase of R123 fluorescence during the late reoxygenation phase (Fig. 5). As shown in Fig. 5B, there is only a minimal late secondary increase of the R123 signal with the short hypoxia (to the left), whereas with the prolonged hypoxia there is much larger secondary increase (middle response). This late increase in R123 fluorescence may be related to hyperoxidation occurring with mitochondrial overactivity during the recovery phase, following reoxygenation. The late increase of R123 fluorescence was also accompanied by a further decrease in IOS, suggesting profound tissue changes following this severe, prolonged hypoxia. However, in this series of experiments, we focused on the short-term changes with hypoxia, and further experiments will be required to determine whether or not a clear relationship exists between hypoxia duration and the amplitude of the late R123 elevation during the late reoxygenation phase. This relationship may clarify the time course of late mitochondrial and neuronal damage following reoxygenation.

#### Hypoxia in $Ca^{2+}$ -free medium

Hippocampal slices have been previously found to recover from prolonged (9 min) hypoxia (and HSD) experienced in  $Ca^{2+}$ -free media, whereas slices in medium with normal  $Ca^{2+}$  concentration failed to recover after a similar prolonged hypoxia (Balestrino and Somjen 1986). It has also been demonstrated that high concentration of free cytosolic  $Ca^{2+}$  can induce mitochondrial depolarization in neurons (Dubinsky and Levi 1998; Loew et al. 1994). These findings suggest that the likely large influx of extracellular  $Ca^{2+}$  associated with hypoxia and HSD might be in part responsible for the induction of the observed profound mitochondrial depolarization. To prevent the large  $Ca^{2+}$  influx, hypoxia experiments were performed as described in the preceding text, with imaging of R123 fluorescence and IOS but in  $Ca^{2+}$ -free medium (no  $Ca^{2+}$  and 1 mM EGTA added). To assess whether the media had the expected physiological effect, we routinely monitored extracellular synaptic responses in the CA1 region; the  $Ca^{2+}$ -free medium reliably resulted in complete loss of the synaptic signal within 5–10 min.

We compared R123 responses during successive HSD episodes induced with hypoxia first in normal and then in  $Ca^{2+}$ -free ACSF in the same slices ( $n = 3$  experiments). The time to onset of HSD did not change significantly in the  $Ca^{2+}$ -free media, and the actual HSD appeared similar electrophysiologically. In addition,  $Ca^{2+}$  withdrawal did not lead to any significant change of the R123 signals, including maxima or slope of the initial and HSD phases (see Fig. 6). Since  $Ca^{2+}$  influx is markedly reduced in these conditions, these results imply that most of the mitochondrial depolarization observed is not directly dependent on an elevation of  $Ca^{2+}$  via  $Ca^{2+}$  influx. However, release of  $Ca^{2+}$  from internal  $Ca^{2+}$  stores could potentially account for at least a partial  $Ca^{2+}$  induction of the mitochondrial depolarization. Additionally the lack of oxygen for mitochondrial respiration may be the key factor leading to the mitochondrial depolarization during the peak of the HSD rather than necessarily  $Ca^{2+}$  influx.

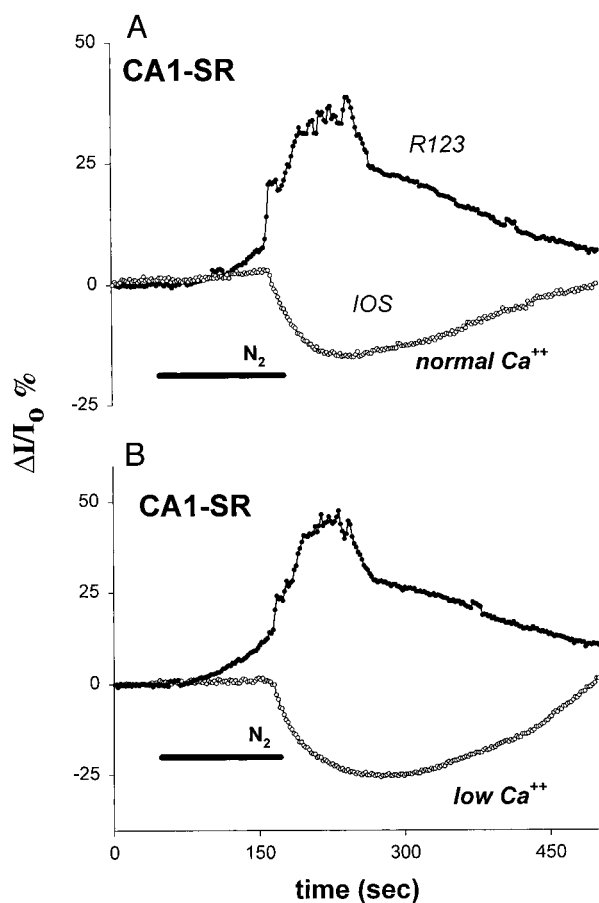


FIG. 6. R123 fluorescence (closed circles) and transmitted light intensity (open circles) in a bath containing normal (1.2 mM) calcium (A) and in calcium-free solution (B). The signals were recorded from the same region of interest in the same slice with 40 min between the 2 frames (solution was switched to calcium-free solution 10 min after the end of the trace shown in A). The ordinate shows the change of fluorescence or transmittance intensity ( $\Delta I$ ) as a percentage of the control level  $I_0$ . Horizontal bars indicate the periods of hypoxia. This figure was obtained using epi-fluorescence.

#### Hypoxia in low-chloride medium

It has recently been shown (Müller and Somjen 1999) that the sharp increase in light scattering associated with hypoxic spreading depression (the IOS described here) is dependent on  $[Cl^-]_o$ . Mechanisms other than cell swelling may account for the complex series of IOS changes described with hypoxia, particularly the anomalous signal with HSD. Mitochondrial (or other organelle) swelling is another possible mechanism. Since mitochondrial swelling can be associated with depolarization of the mitochondrial inner membrane, we have studied the R123 response during HSD induced in low  $Cl^-$  medium. Figure 7 shows plots of R123 and IOS response as measured in s. radiatum of CA1 successively under control (A) and low-chloride (B) conditions in the same slice. The slope of the sharp increase in R123 fluorescence (at HSD onset) was significantly reduced when hypoxia was applied to the same slice, but in medium containing only 2.4 mM  $Cl^-$  (as  $CaCl_2$ ) (Fig. 7B). The data from paired (normal/low  $Cl^-$ ) hypoxic trials revealed that the R123 HSD slope was  $3.14 \pm 1.78$  ( $n = 8$  trials in  $n = 5$  slices) times steeper in normal compared to low  $Cl^-$  ASCF ( $P < 0.01$ ), but the same calculation for pre-SD slopes  $-1.05 \pm 0.65$  did not realize significance between the two conditions. In agreement with the finding of Müller and Somjen (1999), the

sharp decrease in light transmittance with HSD onset was abolished in the low-chloride condition, instead demonstrating a large and rapid increase in transmittance. However, the pre-HSD phase of the IOS persisted unchanged, indicating that this phase (and possibly also the early and late reoxygenation phases) was unaffected by the low- $Cl^-$  media, in contrast to the HSD phase reversal. The significant diminution of the R123 HSD response and reversal of the IOS during the HSD phase strongly suggests that the two signals are closely linked to  $Cl^-$  flux, whereas the other phases are less affected and may be relatively independent of  $Cl^-$  flux, either across the cell membrane or the mitochondrial membrane. Alternatively, the low  $Cl^-$  condition may in some manner protect mitochondria, leading to the attenuated slope and reduced maxima in this situation.

#### R123 fluorescence during normoxic spreading depression

Intrinsic optical changes have been observed in tissue experiencing normoxic SD as well as hypoxia and HSD (Aitken et al. 1998, 1999; Basarsky and Feighan 1999; Basarsky et al. 1998; Obeidat and Andrew 1998; Snow et al. 1983). Also, normoxic SD and HSD are similar in electric and ionic responses. To assess the relative degree of mitochondrial stress, we imaged R123 fluorescence and light transmittance during

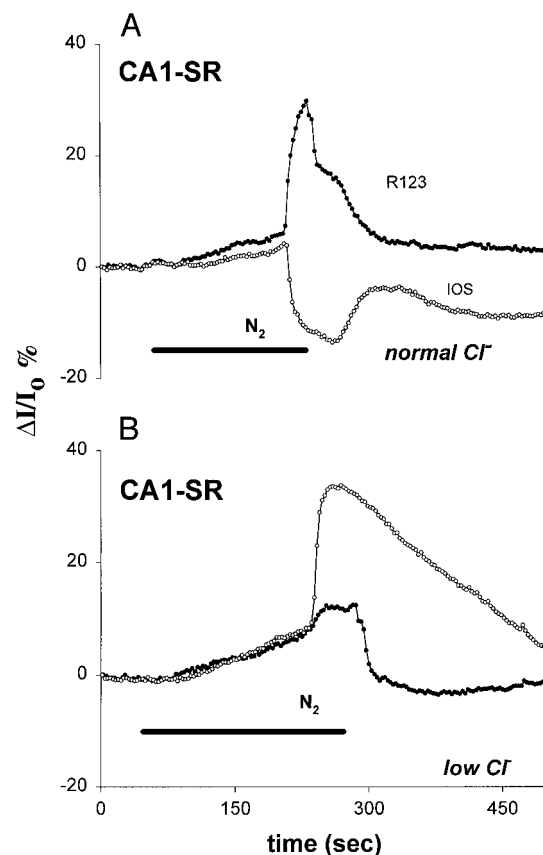


FIG. 7. The effect of low bath  $[Cl^-]$  on the hypoxia-induced changes in R123 fluorescence (closed circles) and light transmittance (open circles). The data for A and for B were obtained from the same slice with an interval of 35 min between the 2 frames (solution was switched to low-chloride solution 6 min after the end of the trace shown in A). The ordinate shows the change of fluorescence or transmittance intensity ( $\Delta I$ ) as a percentage of the control level  $I_0$ . Horizontal bars show the duration of hypoxia. This figure was obtained using transmission fluorescence.

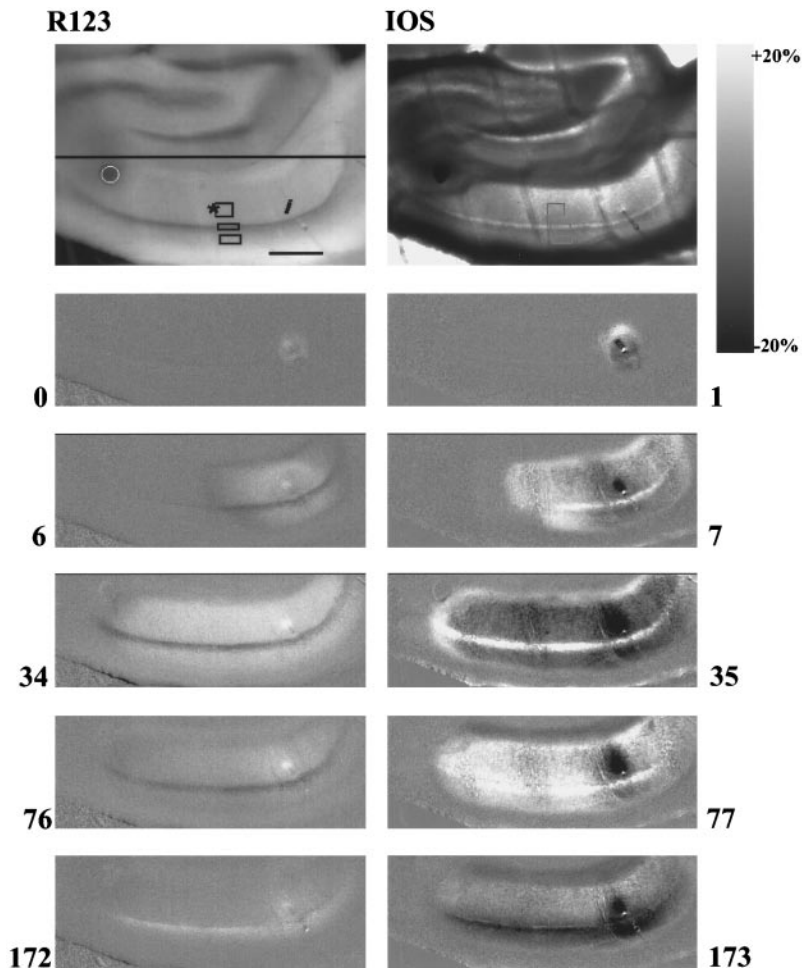


FIG. 8. R123 fluorescence (*left column*) and light transmittance (*right column*) images during an episode of KCl-injection-induced SD. *Top left*: the site of the stimulating electrode is indicated by a small white circle, the extracellular recording electrode by an asterisk, and the regions of optical imaging by rectangles in various layers. The site of the KCl injection is in the lower right of the s. radiatum region, at the end of the slanted line. The bar indicates the region displayed in the remainder of the image sequence, which lies below the bar and is focused in on the CA1 region. The *top 2 frames* show unsubtracted images. The other frames show pixel subtractions as in Fig. 1. The gray scale extends from  $-20\%$  (black) to  $+20\%$  (white). The numbers to the left of the frames show time in seconds after the injection of KCl. This figure was obtained using transmission fluorescence.

normoxic SD induced by micro-injection of KCl. A typical experiment is shown in Fig. 8 as subtracted images and in Fig. 9 as plots of percentage fluorescence change in various ROIs. Micro-injection of 1 M KCl into s. radiatum of CA1 region evoked a propagating wave of SD accompanied by intense IOS

and R123 changes, heralded by the sudden negative shift in extracellular potential ( $\Delta V_o$ ) ( $n = 12$ ). The R123 maximal response averaged  $10.2 \pm 3.1\%$  in CA1 s. radiatum, significantly less than the maximal response noted during HSD. The SD typically propagated through the most of CA1 region but

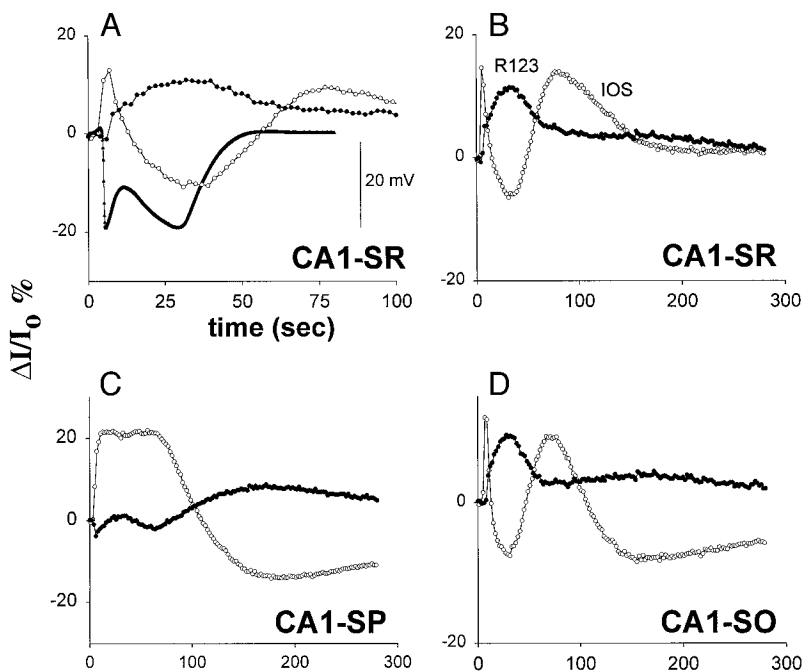


FIG. 9. Changes in mitochondrial membrane potential and IOS during KCl-induced normoxic SD. The percent change in R123 fluorescence intensity (closed circles) and IOS (open circles) were measured in the regions of interest shown in the top left frame of Fig. 8. The KCl injection was performed just after the beginning of the plots, at *time 0*. *A* and *B*: optical changes shown from the same regions but on different time scales; the extracellular voltage is plotted in *A* only as a solid trace. This figure was obtained using transmission fluorescence.

failed to spread beyond CA1, stopping abruptly at both the CA3 and subicular border (Aitken et al. 1998). As analyzed near the recording electrode location, both optical signals changed simultaneously with  $\Delta V_o$  (see Fig. 9A). R123 fluorescence showed a rapid increase in intensity, following first a brief increase in the IOS signal and coincident with a rapid decrease in IOS. In 11 of 12 experiments, the decrease in IOS was preceded by a brief initial (2–4 s) increase, also reported in earlier works (Aitken et al. 1999; Basarsky et al. 1998). Because optical data were limited by the accuracy permitted by a 2-s inter-image interval for the same parameter (IOS or R123 fluorescence), we cannot reliably determine whether the initial IOS increase truly anticipates the slightly delayed increase in R123 fluorescence. Interesting, the maximal increase in R123 fluorescence, decrease in IOS and decrease of  $V_o$  occurred almost simultaneously. The discrepancy between peak times for the various signals averaged  $1.1 \pm 3.6$ ,  $0.8 \pm 5.1$ , and  $1.9 \pm 3.9$  s for IOS and  $V_o$ , R123 fluorescence and  $V_o$ , and R123 and IOS, respectively ( $n = 12$ ; CA1 s. radiatum, near the recording electrode location) and  $0.2 \pm 4.2$ ,  $-0.6 \pm 6.4$ , and  $-1.7 \pm 3.0$  s for IOS and R123 fluorescence, as measured in s. radiatum, s. pyramidale, and s. oriens, respectively.

Detailed analysis of IOS and R123 fluorescence changes revealed that these parameters did not spread uniformly in all subregions of CA1 (Fig. 9). During SD phase, the reduction in IOS (calculated from the amplitude of the initial increase) and the rise in R123 fluorescence were maximal in s. radiatum and s. oriens but minimal in s. pyramidale. The extent of the IOS decrease and R123 fluorescence increase in s. pyramidale varied significantly from slice to slice, and we found that this discrepancy was likely due to the orientation of the cell body layer with respect to the axis of imaging (that is, perpendicular to the slice surface). Because the width of s. pyramidale is much less than the overall slice thickness ( $\sim 40 \mu\text{m}$  compared with  $400 \mu\text{m}$ ), the optical signal from this layer cannot be completely isolated from the signals of adjacent tissue, particularly if the s. pyramidale is not perpendicular to the slice orientation. If the s. pyramidale is slanted with respect to the slice cut, then imaging along the optical axis will contaminate the s. pyramidale signal with that from adjacent layers. However, the example shown in Figs. 8 and 9 does illustrate the situation where the axis of the cell body layer is parallel to the imaging axis. Here the initial rise in transluence in s. pyramidale was not followed by a decrease as appeared in s. radiatum and s. oriens but instead was maintained at a high level during all SD phases. The recovery phase also differed for the response in CA1 st. pyramidale with a much slower return to baseline than for the dendritic layers. In most other examples, the s. pyramidale response is mixed with that of adjacent layers due to the slant of the layer through the tissue slice.

Recovery began almost simultaneously for optical and electrical signals but proceeded in a more delayed and more complex fashion for IOS and R123 fluorescence than for the extracellular potential. Although  $V_o$  was completely restored within  $\sim 30$ – $50$  s following the peak of the SD, final restoration of IOS and R123 fluorescence was not observed until  $\geq 5$ – $10$  min later. According to the time course and character of changes (similar to hypoxia experiments) several phases of the IOS and R123 fluorescence response with SD can be distinguished, including the SD phase, similar to the HSD phase described above for hypoxia. During the SD phase, there is a

rapid increase in the IOS, followed by a rapid decrease to below the control level, as described in the preceding text. The initial recovery phase after the peak of the SD can be characterized as a secondary fast IOS increase to about the same level as was reached during initial SD peak, concurrent with partial recovery of R123 fluorescence to the level of  $\sim 30\%$  of the maximal response during the SD phase (best observed in Fig. 9, B and D). Duration of this stage did not exceed 1 min. During the next recovery phase, the IOS decreased to values lower than the rest level. The R123 signal often showed a gradual late increase at this point. The extent of this late R123 fluorescence increase strongly correlated with the degree of simultaneous IOS decrease and was most pronounced in s. pyramidale. This phase lasted  $\sim 1.5$ – $2$  min. Final restoration occurred when both IOS and R123 fluorescence recovered to the rest levels, which often extended for 10–12 min, coincident with recovery of the synaptic field potential (not shown). It is important to note that complete recovery of optical and electrical signals occurred after normoxic SD episodes in all experiments (data not shown).

During SD, less mitochondrial depolarization is observed in the cell body layer than in the dendritic layer. However, R123 fluorescence does rise in the post-SD period. The correlation between R123 fluorescence increase and IOS decrease in different regions suggests a definite relationship between the IOS decrease and mitochondrial depolarization during SD. Note, however, that the presence of SD alone generates a mitochondrial depolarization that is small in contrast to that induced by the metabolic stress of hypoxia.

## DISCUSSION

We have demonstrated that mitochondrial membrane potential, measured via R123 fluorescence, and the intrinsic optical signal exhibit multiple phases when hippocampal slices are temporarily made hypoxic. The pre-HSD phase represents a progressive loss of mitochondrial function, leading to depolarization, in response to hypoxia. The HSD phase is similar to that observed during normoxic SD. The R123 fluorescence signal is minimally affected by a lack of external  $\text{Ca}^{2+}$ , whereas decreased external chloride concentration leads to a profound blunting of the R123 response and a reversal of the intrinsic optical signal. Even with extended hypoxia from which slices do not recover electrophysiologically, the R123 fluorescence rapidly recovers on reoxygenation, though with an enhanced later response, suggestive of reoxygenation stress. These various aspects will be discussed in further detail.

### *Phases of R123 fluorescence and intrinsic optical signal response to hypoxia*

Hypoxia of brain tissue *in vitro* proceeds in three epochs. 1) First the membrane potential of many but not all neurons hyperpolarizes due to increased membrane potassium conductance, and synaptic transmission is depressed because voltage-gated  $\text{Ca}^{2+}$  channels fail to open in presynaptic terminals (Hansen 1985; Young and Somjen 1992). 2) This initial epoch is followed by SD-like depolarization, or HSD. Initially, this state, however drastically outside normal physiological limits, is still completely reversible (Hansen 1985; Somjen et al. 1993). 3) If hypoxia continues, neurons become irreversibly injured. Cells can be irreversibly damaged without undergoing

HSD, but the demise of cerebral neurons is greatly accelerated by the massive entry of  $\text{Ca}^{2+}$  ions during HSD. This is shown by the fact that withholding  $\text{Ca}^{2+}$  from the bathing fluid can greatly extend the period of revocability (Balestrino and Somjen 1986; Roberts and Sick 1988) even though HSD is not prevented. Yet the influx of  $\text{Ca}^{2+}$  does not kill neurons instantly; there seems to be a critical minimal period during which high  $[\text{Ca}^{2+}]_o$  must act before it endangers neuron survival.

The data presented in this paper speak to the pathophysiological processes occurring during the first two epochs of hypoxia, which correspond to the five phases of R123 fluorescence and intrinsic optical signals we have described. During the first phase (and epoch 1, prior to HSD onset), we have observed a diffuse, slow initial brightening of the R123 signal over wide areas of the tissue slice, indicating gradual depolarization of mitochondria. This was followed by a sudden increase in R123 fluorescence that spreads as a wave over the tissue, the onset of which at different sites coincided with the onset of a decrease in light transmittance and of the SD-like  $\Delta V_o$  (the HSD epoch or phase 2). Heterogeneity of IOS responses during SD in different regions of hippocampal slice has also been described in earlier works (Aitken et al. 1998; Basarsky et al. 1998; Kreisman and LaManna 1999; Obeidat and Andrew 1998).

During normoxic, KCl-injection-induced SD, we have observed a similar sudden, wave-like increase in R123 fluorescence, concomitant with  $\Delta V_o$ , and a decrease in light transmittance but without the preceding slow fluorescence increase and quantitatively exhibiting a lower level of R123 fluorescence. This suggests that the initial R123 brightening early in hypoxia represents mitochondrial depolarization that is specific to diffuse hypoxic stress, while the sharp, wave-like increase of the R123 signal is directly related to both normoxic and hypoxic SD and the resulting profound metabolic demand imposed on mitochondria for ion pumping needs. This stress would be expected to be much greater with HSD since the tissue has already experienced a profound depletion of oxygen prior to the onset of HSD. The association of these two signals is further underscored by the suppression of both the decrease in light transmittance and the sharp increase of the R123 fluorescence in  $\text{Cl}^-$ -free medium.

We observed a much closer correspondence of the R123 and IOS signals during normoxic SD than in hypoxic SD. This finding is not surprising given the difference between the two conditions. In normoxic SD, the mitochondria are likely responding to a single stress, namely the redistribution of ions that is caused by SD. Since the IOS changes are also caused, directly or indirectly, by this ionic flux, one would expect a good temporal correlation between the two measures. In hypoxia, however, things are much more complex. Mitochondria are responding not only to ionic fluxes but also to oxygen deprivation, redox state changes, and other changes that are a part of hypoxic but not of normoxic SD. Therefore lack of a close temporal correlation between the IOS and R123 signals is to be expected.

In early reports on mitochondrial volume changes, it has been asserted that isotonic mitochondrial swelling can take place if the medium contains "permeant anions" (e.g., Azzone et al. 1976a,b, and previous work quoted by these authors). It is not clear how the substitution of methylsulfate for chloride affects the resting anion composition of the cytosol, but it

undoubtedly prevents the massive influx of  $\text{Cl}^-$  during HSD. For this reason, the chloride dependence of the light scattering increase during HSD seemed to suggest that it may be due directly to the swelling of mitochondria (Müller and Somjen 1999). Clearly, mitochondrial swelling can be only part of the mechanism of IOS changes, as evidenced by the frequent discrepancies between the IOS and R123 signals in our experiments. It is important to keep in mind the fact that R123 measures mitochondrial membrane potential, not swelling, and while swelling and depolarization are often closely correlated, they are not the same thing. Mitochondrial depolarization is frequently, though not invariably, associated with mitochondrial swelling. Thus the chloride dependence of the sharp, wave-like increase of the R123 signal (phase 2) agrees with the idea that it, as well as the transmittance decrease of the IOS, is in some way related to mitochondrial swelling. This conclusion is further supported by the distribution of the IOS and R123 signals, both of which are much more pronounced in regions rich in mitochondria, such as the neuropil, than in mitochondria-poor layers, as s. pyramidale (Bindokas et al. 1998; Nafstad and Blackstad 1966). Yet the sharp increase of R123 fluorescence sometimes could invade areas that did not demonstrate an IOS, and which are relative resistant to HSD (shown in Figs. 3 and 4) (Balestrino et al. 1989; Basarsky et al. 1998; Kawasaki et al. 1990). It seems that, while SD-like depolarization invariably leads to severe depolarization of mitochondria, mitochondrial depolarization can occur without the SD-like change and, inferentially, without mitochondrial swelling. A problem with this train of thought is the well-known fact that in suspensions of isolated mitochondria, swelling of these organelles is accompanied by decreased light scattering (increased transmittance) (Raaflaub 1953). Our suggestion rests on the assumption that within cells, the refractive index of the mitochondria may differ from that of the cytosol, in which case an expansion of their surface would increase scattering. Clearly this issue is not settled. Among other reasons for changes in tissue scattering and light transmittance may be changes in the aggregation of macromolecules. Thus while there are several possible mechanisms for the discrepancy between the increased light transmittance noted during the early phase of hypoxia and the profound decreased transmittance observed during the peak of HSD and normoxic SD, the swelling of intracellular organelles may be an important aspect of these SD-related signals.

There is ample evidence for a correlation between the duration of HSD and hypoxic neuron injury (Adachi et al. 1998; Balestrino 1995; Balestrino and Somjen 1986; Balestrino et al. 1999; Lee and Lowenkopf 1993; Tombaugh 1994; Watson and Lanthorn 1995). The uptake of  $\text{Ca}^{2+}$  into neurons is a critical event in the injury (Balestrino and Somjen 1986; Roberts and Sick 1988; Siesjö and Bengtsson 1989). Since elevated  $[\text{Ca}^{2+}]_i$  triggers the mitochondrial permeability transition (mPT) and this transition depolarizes mitochondria and impairs their function (Crompton 1999; Gunter et al. 1994; Lemasters et al. 1997; Loew et al. 1994), we have asked whether the influx of  $\text{Ca}^{2+}$  is required for the sharp increase of R123 fluorescence. The answer to this question was negative: withdrawing  $\text{Ca}^{2+}$  from the preparation did not prevent the sudden mitochondrial depolarization. While our data do not address the question of neuronal survival, it seems that the injury by excessive intracellular  $\text{Ca}^{2+}$  is not due directly to mitochondrial depolarization but rather to the catalysis of some other biochemical

process leading to cell autolysis (Siesjö 1981; Siesjö and Bengtsson 1989).

However, there is a discrepancy between prolonged, irreversible hypoxia (in terms of slice recovery) and the rapid repolarization of mitochondria with reoxygenation, suggesting that mitochondria may remain viable far beyond neuronal survival. In addition, the late increase in R123 fluorescence (late reoxygenation phase) may represent a form of reoxygenation damage to mitochondria (Leyssens et al. 1996). This type of mitochondrial stress evident on reoxygenation has also been attributed to hyperoxidation since the rapid return of oxygen may in itself damage electron transport in mitochondria through overactivation (Pérez-Pinzón et al. 1998). However, the appearance of a small secondary increase in R123 fluorescence even after KCl-injection-induced SD suggests that there may be other explanations as well. Qualitatively, the degree of the late reoxygenation elevation in R123 fluorescence appeared to be correlated with the duration of hypoxia, particularly following HSD, and further studies may be helpful in assessing this potential correlation.

#### *Does the large R123 change represent a mitochondrial permeability transition?*

It is not clear whether the sharp increase of R123 fluorescence represents mPT or some other mechanism of mitochondrial depolarization. The opening of the permeability pores can be a prelude to irreversible injury (Gunter et al. 1994; Lemasters et al. 1997), yet the hippocampal slices do recover electrophysiological function after short periods of HSD and the associated large change in R123 fluorescence. Recently it has become clear, however, that transient, low-conductance mPT can also occur during normal function (Ichas et al. 1997). Likewise even after prolonged hypoxia, there is still a rapid decrease in R123 fluorescence with reoxygenation, indicating that mitochondria can still sequester R123 during and/or after repolarization and arguing against any form of irreversible mitochondrial injury. Moreover, Müller and Somjen (1999) found that the administration of cyclosporin-A did not prevent the SD-like IOS response (though there may be some doubt about permeation of the cyclosporin into slices). None of these observations are completely decisive, but, for now, it seems more probable that the SD-related sharp depolarization of mitochondria is due to some mechanism other than the opening of the permeability transition pore. For example, loss of oxygen as a critical mitochondrial substrate may in itself serve to cause the observed depolarization, and this explanation would be consistent with the observed rapid recovery of the R123 fluorescence signal with reoxygenation.

#### *Usefulness of R123 fluorescence in slices*

Although slices exhibited variable loading of the R123 dye, the qualitative response and phases we have described were consistent between slices. Clearly loading of mitochondria in slices represents both those from both glial and neuronal elements, and single-cell studies will be required to assess the relative contribution of individual cell types to these phases of hypoxia-induced signals. The fluorescence was robust and was detected using both epifluorescence and transmission fluorescence techniques, and with a range of excitation/emission filter sets (though still appropriate to the dye wavelengths). Surpris-

ingly, there appeared to be neither significant bleaching or fade with prolonged signal elevations and there was minimal leaching from cells with mitochondrial depolarization. The R123 signal was appreciably more rapid in response than the IOS, which usually was delayed following a sudden tissue change, such as with SD occurrence. The fluorescence responded appropriately to critical control conditions, particularly FCCP, so mitochondrial localization similar to that of other *in vitro* preparations, such as tissue culture, appears an appropriate assumption. Thus R123 shows a rapid response and a high degree of fluorescence and appears to be specific to mitochondrial depolarization, from critical previous studies of mitochondrial function. However, the linkage between R123 fluorescence and mitochondrial membrane states, such as the permeability transition, remain unclear, and further types of mitochondrial-specific dyes may be needed to more fully delineate the presence or absence of such a large transition with HSD and SD occurrence.

We thank Dr. Michael Müller for suggestions and a critical reading of the manuscript.

This work was supported by National Institutes of Health Grants NS-18670 and AG-13165 and a Veterans Affairs Merit Review Award.

#### REFERENCES

- ADACHI N, CHEN J, LIU K, TSUBOTA S, AND ARAI T. Dexamethasone aggravates ischemia-induced neuronal damage by facilitating the onset of anoxic depolarization and the increase in the intracellular  $Ca^{++}$  concentration in gerbil hippocampus. *J Cereb Blood Flow Metab* 18: 274–280, 1998.
- AITKEN PG, FAYUK D, SOMJEN GG, AND TURNER DA. Use of intrinsic optical signals to monitor physiological changes in brain tissue slices. *Compan Methods Enzymol* 18: 91–103, 1999.
- AITKEN PG, TOMBAUGH GC, TURNER DA, AND SOMJEN GG. Similar propagation of SD and hypoxic SD-like depolarization in rat hippocampus recorded optically and electrically. *J Neurophysiol* 80: 1514–1521, 1998.
- AZZONE GF, MASSARI S, AND POZZAN T. Mechanism of active shrinkage in mitochondria. I. Coupling between weak electrolyte fluxes. *Biochim Biophys Acta* 423: 15–26, 1976a.
- AZZONE GF, MASSARI S, AND POZZAN T. Mechanism of active shrinkage in mitochondria. II. Coupling between strong electrolyte fluxes. *Biochim Biophys Acta* 423: 27–41, 1976b.
- BALESTRINO M. Pathophysiology of anoxic depolarization: new findings and a working hypothesis. *J Neurosci Methods* 59: 99–103, 1995.
- BALESTRINO M, AITKEN PG, AND SOMJEN GG. Spreading depression-like hypoxic depolarization in CA1 and fascia dentata of hippocampal slices: relationship to selective vulnerability. *Brain Res* 497: 102–107, 1989.
- BALESTRINO M, REBAUDO R, AND LUNARDI G. Exogenous creatine delays anoxic depolarization and protects from hypoxic damage: dose-effect relationship. *Brain Res* 816: 124–130, 1999.
- BALESTRINO M AND SOMJEN GG. Chlorpromazine protects brain tissue in hypoxia by delaying spreading depression-mediated calcium influx. *Brain Res* 385: 219–229, 1986.
- BASARSKY TA, DAFFY SN, ANDREW RD, AND MACVICAR, BA. Imaging spreading depression and associated intracellular calcium waves in brain slices. *J Neurosci* 18: 7189–7199, 1998.
- BASARSKY TA AND FEIGHAN D. Glutamate release through volume-activated channels during spreading depression. *J Neurosci* 19: 6439–6445, 1999.
- BINDOKAS VP, LEE CC, COLMERS WF, AND MILLER RJ. Changes in mitochondrial function resulting from synaptic activity in the rat hippocampal slice. *J Neurosci* 18: 4570–4587, 1998.
- CHOI DW. Calcium-mediated neurotoxicity: relationship to specific channel type and role in ischemic damage. *Trends Neurosci* 11: 465–469, 1988.
- CROMPTON M. The mitochondrial permeability transition pore and its role in cell death. *Biochem J* 341: 233–249, 1999.
- DAVID G, BARRETT JN, AND BARRETT EF. Evidence that mitochondria buffer physiological  $Ca^{2+}$  loads in lizard motor nerve terminals. *J Physiol (Lond)* 509: 59–65, 1998.
- DUBINSKY JM AND LEVI Y. Calcium-induced activation of the mitochondrial permeability transition in hippocampal neurons. *J Neurosci Res* 53: 728–741, 1998.

- DUCHEN MR.  $\text{Ca}^{2+}$ -dependent changes in the mitochondrial energetics in single dissociated mouse sensory neurons. *Biochem J* 283: 41–50, 1992.
- EBINE Y, FUJIWARA N, AND SHIMOJI K. Mild acidosis inhibits the rise in intracellular  $\text{Ca}^{++}$  concentration in response to oxygen-glucose deprivation in rat hippocampal slices. *Neurosci Lett* 168: 155–158, 1994.
- GROUSELLE M, TUEUX O, DABADIE P, GEORGESCAUD D, AND MAZAT JP. Effect of local anaesthetics on mitochondrial membrane potential in living cells. *Biochem J* 271: 269–272, 1990.
- GRØNDAHL TO AND LANGMOEN IA. Cytotoxic effect of  $\text{Ca}^{2+}$  released from intracellular stores during cerebral energy deprivation. *Neurol Res* 18: 499–504, 1996.
- GUNTER TE, GUNTER KK, SHEU SS, AND GAVIN CE. Mitochondrial calcium transport: physiological and pathological relevance. *Am J Physiol Cell Physiol* 267: C313–C339, 1994.
- HANSEN AJ. Effects of anoxia on ion distribution in the brain. *Physiol Rev* 65: 101–148, 1985.
- HEYTLER PG. Uncouplers of oxidative phosphorylation. *Pharmacol Therap* 10: 461–472, 1980.
- HULSMANN S, GREINER C, KOHLING R, WOLFER J, MOSKOPP D, RIEMANN B, LUCKE A, WASSMANN H, AND SPECKMANN EJ. Dimethyl sulfoxide increases latency of anoxic terminal negativity in hippocampal slices of guinea pig in vitro. *Neurosci Lett* 261: 1–4, 1999.
- ICHAS F, JOUAVILLE LS, AND MAZAT JP. Mitochondria are excitable organelles capable of generating and conveying electrical and calcium signals. *Cell* 89: 1145–1153, 1997.
- JING J, AITKEN PG, AND SOMJEN GG. Role of calcium channels in spreading depression in rat hippocampal slices. *Brain Res* 604: 251–259, 1993.
- JOHNSON LJ, CHUNG W, HANLEY DF, AND THAKOR NV. Optical scatter imaging of mitochondrial and cellular swelling in the hippocampal slice. *Soc Neurosci Abstr* 24: 1129, 1998.
- JOHNSON LV, WALSH ML, BOCKUS BJ, AND CHEN LB. Monitoring of relative mitochondrial membrane potential in living cells by fluorescence microscopy. *J Cell Biol* 88: 526–535, 1981.
- KASS I AND LIPTON P. Mechanisms involved in irreversible anoxic damage to the in vitro rat hippocampal slice. *J Physiol (Lond)* 332: 459–472, 1982.
- KAWASAKI K, TRAYNELIS SF, AND DINGELDINE R. Different responses of CA1 and CA3 to hypoxia in rat hippocampal slice. *J Neurophysiol* 63: 385–394, 1990.
- KREISMAN NR AND LAMANNA JC. Rapid and slow swelling during hypoxia in the CA1 region of rat hippocampal slices. *J Neurophysiol* 82: 320–329, 1999.
- KREISMAN NR, LAMANNA JC, LIAO, S-C, AND ALCALA JR. Hypoxia-induced changes in light transmittance in hippocampal slices. *Soc Neurosci Abstr* 20: 1040, 1994.
- KRISTAL BS AND DUBINSKY JM. Mitochondrial permeability transition in the central nervous system: induction by calcium-cycling dependent and independent pathways. *J Neurochem* 69: 524–538, 1997.
- KRISTIÁN T AND SIESJÖ BK. Calcium-related damage in ischemia. *Life Sci* 59: 357–367, 1996.
- LEÃO AAP. Spreading depression of activity in the cerebral cortex. *J Neurophysiol* 7: 359–390, 1944.
- LEÃO AAP. Further observations on the spreading depression of activity in the cerebral cortex. *J Neurophysiol* 10: 409–414, 1947.
- LEE KS AND LOWENKOPF T. Endogenous adenosine delays the onset of hypoxic depolarization in the rat hippocampus in vitro via an action at A1 receptors. *Brain Res* 609: 313–315, 1993.
- LEMASTERS JJ, NIEMINEN AL, QIAN T, TROST LC, AND HERMAN B. The mitochondrial permeability transition in toxic, hypoxic and reperfusion injury. *Mol Cell Biochem* 174: 159–165, 1997.
- LEYSSENS A, NOWICKY AV, PATTERSON L, CROMPTON M, AND DUCHEN MR. The relationship between mitochondrial state, ATP hydrolysis,  $[\text{Mg}^{2+}]$ , and  $[\text{Ca}^{2+}]$ , studied in isolated rat cardiomyocytes. *J Physiol (Lond)* 496: 111–128, 1996.
- LOEW LM, CARRINGTON W, TUFT RA, AND FAY FS. Physiological cytosolic  $\text{Ca}^{2+}$  transients evoke concurrent mitochondrial depolarizations. *Proc Natl Acad Sci USA* 91: 12579–12583, 1994.
- MATYJA E AND KIDA E. Hippocampal damage in vitro after different periods of oxygen deprivation. *Neuropatol Polska* 30: 231–243, 1992.
- MITANI A, TAKEYASU S, YANASE H, NAKAMURA Y, AND KATAOKA K. Changes in intracellular  $\text{Ca}^{++}$  and energy levels in the gerbil hippocampal slice. *J Neurochem* 62: 626–634, 1994.
- MÜLLER M AND SOMJEN GG. Inhibition of major cationic inward currents prevents spreading depression-like hypoxic depolarization in rat hippocampal tissue slices. *Brain Res* 812: 1–13, 1998.
- MÜLLER M AND SOMJEN GG. Intrinsic optical signals in rat hippocampal slices during hypoxia-induced spreading depression-like depolarization. *J Neurophysiol* 82: 1818–1831, 1999.
- NAFSTAD HJ AND BLACKSTAD TW. Distribution of mitochondria in pyramidal cells and boutons in hippocampal cortex. *Z Zellforsch Mikrosk Anat* 73: 234–245, 1966.
- NICHOLLS DG. A role for the mitochondrion in the protection of cells against calcium overload? *Prog Brain Res* 63: 97–106, 1985.
- NICHOLSON C AND KRAIG RP. The behavior of extracellular ions during spreading depression. In: *The Application of Ion-Selective Microelectrodes*, edited by Zeuthen T. Amsterdam: Elsevier, 1981, p. 217–238.
- OBEIDAT AS AND ANDREW RD. Spreading depression determines acute cellular damage in the hippocampal slice during oxygen/glucose deprivation. *Eur J Neurosci* 10: 3451–3461, 1998.
- PÉREZ-PINZÓN M, MUMFORD PL, AND SICK TJ. Prolonged anoxic depolarization exacerbates NADH hyperoxidation and promotes poor electrical recovery after anoxia in hippocampal slices. *Brain Res* 786: 165–170, 1998.
- RAAFLAUB J. Die Schwellung isolierter Lebermitochondrien und ihre physikalisch-chemische Beeinflussbarkeit. *Helv Physiol Pharmacol Acta* 11: 142–156, 1953.
- ROBERTS EL AND SICK TJ. Calcium-sensitive recovery of extracellular potassium and synaptic transmission in rat hippocampal slices exposed to anoxia. *Brain Res* 456: 113–119, 1988.
- SHIHO A, MATSUDA M, HANADA J, AND CHANCE B. Poor recovery of mitochondrial redox state in CA1 after transient forebrain ischemia in gerbils. *Stroke* 29: 2421–2425, 1998.
- SIESJÖ BK. Cell damage in the brain: a speculative synthesis. *J Cereb Blood Flow Metab* 1: 155–185, 1981.
- SIESJÖ BK AND BENGTTSSON F. Calcium fluxes, calcium antagonists, and calcium-related pathology in brain ischemia, hypoglycemia, and spreading depression: a unifying hypothesis. *J Cereb Blood Flow Metab* 9: 127–140, 1989.
- SILVER IA AND ERECIŃSKA M. Intracellular and extracellular changes of  $[\text{Ca}^{2+}]$  in hypoxia and ischemia in rat brain in vivo. *J Gen Physiol* 95: 837–866, 1990.
- SIMS NR. Calcium, energy metabolism and the development of selective neuronal loss following short-term cerebral ischemia. *Metab Brain Dis* 10: 191–217, 1995.
- SNOW RW, TAYLOR CP, AND DUDEK FE. Electrophysiological and optical changes in slices of rat hippocampus during spreading depression. *J Neurophysiol* 50: 561–572, 1983.
- SOMJEN GG AND AITKEN PG. The ionic and metabolic responses associated with neuronal depression of Leao's type in cerebral cortex and in hippocampal formation. *An Acad Brasil Cien* 56: 495–504, 1984.
- SOMJEN GG, AITKEN PG, BALESTRINO M, HERRERAS O, AND KAWASAKI K. Spreading depression-like depolarization and selective vulnerability of neurons: a brief review. *Stroke* 21: 179–183, 1990.
- SOMJEN GG, HERRERAS O, AND JING J. Spreading depression and neuron damage: a brief review. *Exp Brain Res Ser* 23: 27–33, 1992.
- SOMJEN GG, AITKEN PG, CZECH G, JING J, AND YOUNG JN. Cellular physiology of hypoxia of the mammalian central nervous system. In: *Molecular and Cellular Approaches to the Treatment of Neurological Disease*, edited by Waxman SG. New York: Raven, 1993, p. 51–65.
- SWEENEY MI, YAGER JY, WALZ W, AND JUURLINK BH. Cellular mechanisms involved in brain ischemia. *Can J Physiol Pharmacol* 73: 1525–1535, 1995.
- TANAKA E, YAMAMOTO S, KUDO Y, MIHARA S, AND HIGASHI H. Mechanisms underlying the rapid depolarization produced by deprivation of oxygen and glucose in rat hippocampal neurons in vitro. *J Neurophysiol* 78: 891–902, 1997.
- TOMBAUGH GC. Mild acidosis delays hypoxic spreading depression and improves neuronal recovery in hippocampal slices. *J Neurosci* 14: 5635–5643, 1994.
- TURNER DA, AITKEN PG, AND SOMJEN GG. Optical mapping of translucence changes in rat hippocampal slices during hypoxia. *Neurosci Lett* 195: 209–213, 1995.
- WATSON GB AND LANTHORN TH. Phenytoin delays ischemic depolarization, but cannot block its long-term consequences, in the rat hippocampal slice. *Neuropharmacology* 34: 553–558, 1995.
- YAMAMOTO S, TANAKA E, SHOJI Y, KUDO Y, INOKUCHI H, AND HIGASHI H. Factors that reverse the persistent depolarization produced by deprivation of oxygen and glucose in rat hippocampal CA1 neurons in vitro. *J Neurophysiol* 78: 903–911, 1997.
- YOUNG JN AND SOMJEN GG. Suppression of presynaptic calcium currents by hypoxia in hippocampal tissue slices. *Brain Res* 573: 70–76, 1992.
- ZHANG Y AND LIPTON P. Cytosolic  $\text{Ca}^{2+}$  changes during in vitro ischemia in rat hippocampal slices: major roles for glutamate and  $\text{Na}^{+}$ -dependent  $\text{Ca}^{2+}$  release from mitochondria. *J Neurosci* 19: 3307–3315, 1999.